

RESEARCH

Open Access



# Increased pro-SFTPB in HDL promotes the pro-inflammatory transition of HDL and represents a sign of poor prognosis in ARDS patients

Liu Yang<sup>1,2†</sup>, Zhuo Xu<sup>1†</sup>, Zhenyan Wang<sup>2,3</sup>, Fangping Ding<sup>1</sup>, Zhipeng Wu<sup>1</sup>, Xiaoqian Shi<sup>2,3</sup>, Jing Wang<sup>2</sup>, Yingmin Ma<sup>1\*</sup> and Jiawei Jin<sup>2,3\*</sup>

## Abstract

**Background** Acute respiratory distress syndrome (ARDS) is causatively associated with excessive alveolar inflammation involving deregulated pro-inflammatory macrophage polarization. High-density lipoprotein (HDL) showed critical anti-inflammatory roles by modulating macrophage function, and its adverse transition to pro-inflammation has an important role in the pathogenesis of ARDS. However, the relationship between HDL protein constituents and functional remodeling is unknown in ARDS.

**Methods** Proteomic techniques were applied to examine the protein profile changes in HDL from septic-ARDS patients versus HDL from healthy controls across two distinct cohorts: a discovery cohort (8 patients and 8 healthy controls) and a validation cohort (22 patients and 10 healthy controls). The changed components significantly associated with prognosis were identified. Luminex assessed the levels of 38 plasma cytokines and chemokines. The in vitro constructed pro-SFTPB enriched HDL was applied to confirm the effect on M1 polarization of THP1-derived macrophage.

**Results** 18 proteins were validated from 102 changed HDL proteins identified in the discovery cohort, including HDL particle components, such as apolipoproteins, pro-inflammatory substances known as serum amyloid As (SAAs), and anti-oxidative proteins like paraoxonases (PONs). Among these proteins, only the increase of pro-SFTPB in HDL was significantly associated with poor prognosis of ARDS patients. Notably, HDL-pro-SFTPB level was correlated with plasma pro-inflammatory cytokines and chemokines levels. The correlation assay of pro-SFTPB with other HDL components showed that it was positively and negatively correlated with SAA2 and PON3, respectively. Furthermore, the in vitro studies confirmed that the pro-SFTPB enriched HDL significantly promoted M1 polarization of monocyte-derived macrophages.

<sup>†</sup>Liu Yang and Zhuo Xu are Co-first author.

\*Correspondence:

Yingmin Ma  
mayingmin@ccmu.edu.cn  
Jiawei Jin  
jiaweijin@ccmu.edu.cn

Full list of author information is available at the end of the article



**Conclusions** The increase of HDL-pro-SFTPb promotes HDL pro-inflammatory transition during septic ARDS, leading to exacerbated progression of ARDS through enhancing M1 macrophage polarization. HDL-pro-SFTPb could be a useful prognostic biomarker for septic ARDS.

**Keywords** ARDS, Sepsis, Pro-SFTPb, HDL proteomics, Macrophage

## Background

Acute respiratory distress syndrome (ARDS), as a prevalent fatal consequence of severe pneumonia and sepsis, is characterized by acute respiratory failure due to diffuse pulmonary inflammatory injury and edema [1]. During pulmonary inflammatory response, the polarization of macrophages toward pro-inflammatory M1 is critical for innate immune defenses because of their phagocytic function and macrophage-derived cytokines [2]. However, deregulated M1 macrophage polarization causes excessive alveolar inflammation and alveolar damage, finally leading to ARDS [3, 4]. Moreover, during the resolution of lung injury, these cells repolarize toward anti-inflammatory M2 macrophages expressing reparative markers [5]. In ARDS patients, persistent M1 polarization has been shown as a strong predictor of poor prognosis [6]. Therefore, the clinical relevance of understanding novel modulating monocyte-derived macrophage polarization during ARDS is crucial for exploring novel biomarkers and therapeutic targets.

High-density lipoprotein (HDL) showed critical protective roles in modulating macrophage function due to its anti-inflammatory, anti-oxidative properties and cholesterol efflux capacities [7, 8]. The pretreatment of HDL inhibits the M1 polarization of human monocyte-derived macrophages, accompanied by a decrease in pro-inflammatory gene expression and reactive oxygen species (ROS) production [9]. The clinic relevance studies demonstrate that decreased plasma HDL cholesterol (HDL-C) is significantly associated with adverse prognosis in patients with severe sepsis and ARDS [10, 11]. Furthermore, increasing studies indicate an adverse transition of HDL to pro-inflammation in acute inflammatory disorder diseases, including sepsis and ARDS, which is associated with HDL composition and structural remodeling [12–15]. Although the detrimental HDL transition was highlighted in the pathogenesis of septic-ARDS, the remodeling in HDL constituents during ARDS is largely unknown.

HDL, as a heterogeneous particle, contains distinct components of proteins involved in lipid transport, innate immunity, inflammation, cell adhesion, hemostasis, protease regulation, and even vitamin and metal binding [16, 17]. The proteomic studies on cardiovascular diseases and diabetes demonstrated that HDL protein components are modified accompanied by functional

transition, including apolipoproteins (apos), paraoxonases (PONs), and serum amyloid As (SAAs) [14, 18–20]. Furthermore, our previous study found that HDL from septic-ARDS patients exhibits pro-inflammatory transition with reduced apoA-I and increased apoC-III, apoE, and SAA, suggesting that the HDL protein constituents change would play an essential role in functional transition during ARDS [15]. However, no proteomic study has elucidated HDL protein profile changes in ARDS patients.

In this study, we applied proteomic techniques to explore the protein profile changes in HDL from septic-ARDS patients versus HDL from healthy controls. The significantly changed protein components were further confirmed in a validation cohort, including apos, PONs, insulin-like growth factor-binding protein 3 (IGFBP3), serpin family A member 5 (SERPIN5), lipopolysaccharide-binding protein (LBP), pro-pulmonary surfactant-associated protein B (pro-SFTPb) and SAAs. Among these proteins, the increase of pro-SFTPb in HDL is significantly associated with poor prognosis of ARDS patients, and it was correlated with the levels of plasma cytokines and chemokine in the validation cohort. Of note, the linear regression assay also showed pro-SFTPb in HDL could capture a positive effect on the pro-inflammatory component SAA2 and a negative effect on the anti-oxidative component PON3. Furthermore, pro-SFTPb enriched HDL in vitro constructed by using normal HDL and recombinant pro-SFTPb protein significantly promoted M1 polarization of monocyte-derived macrophage, which provided direct evidence for the importance of pro-SFTPb in HDL pro-inflammatory remodeling. These findings indicate the importance of increased HDL-pro-SFTPb in HDL pro-inflammatory transition during ARDS, leading to exacerbated progression of septic-ARDS through enhancing M1 macrophage polarization.

## Methods

### Subjects and samples

The cohort study enrolled adult septic-ARDS patients (ages  $\geq 18$  years) meeting the criteria of Sepsis-3 and ARDS Berlin definition, and receiving invasive mechanical ventilation (IMV) treatment from the respiratory intensive care unit (RICU). Their plasma samples were

obtained within 24 h after ARDS confirmation. The patients were excluded as follows: patients who died within 3 days; patients with diabetes mellitus or hypercholesterolemia; patients who received lipid-modifying therapies (statin drugs use); pregnant women; inability to obtain informed consent. Moreover, adult healthy volunteers from the health examination center of Beijing Chaoyang Hospital were included. All subjects or their representatives signed the informed consent. This study was approved by the Ethics Committee of Beijing Chaoyang Hospital (approval No.: 2021-ke-313) and Beijing You-an Hospital (approval No.: LL-2021-148-K).

#### Data collection

Demographic and clinical data like age, sex, body mass index (BMI), underlying diseases, etiology, acute physiology and chronic health evaluation II (APACHE II) score, sequential organ failure assessment (SOFA) score, laboratory data at admission, complications, treatment during RICU and prognosis were collected. Patients were divided into a survivor group and a non-survivor group based on ARDS-related mortality within 28 days after admission.

#### HDL isolation

HDL (density 1.063–1.210 g/ml) was isolated from plasma by discontinuous density gradient ultracentrifugation as previously described [21]. For data-independent acquisition mass spectrometry (DIA-MS) proteomic assay, the plasma from 2 individuals with similar demographic and clinical situations (including age, sex, BMI, underlying diseases, etiology, APACHE II score, SOFA score and prognosis) were pooled to identify changed HDL components efficiently. The purity of HDL was confirmed by the 10% SDS-PAGE electrophoresis and immunoblot of apoA-I (Santa Cruz, sc-376818) and apoB (Sigma, AB742) (Supplemental Figure 1).

#### Cytokine measurement

Plasma levels of 38 cytokines were quantified by Luminex multiplex bead-based assay using MILLIPLEX<sup>®</sup> MAP Human Cytokine/Chemokine/Growth Factor Panel (Merck Millipore, HCYTA-60 K), according to the manufacturer's protocols.

#### DIA-MS proteomic analysis

##### Sample preparation

The HDLs were centrifugated for 10 min at 12,000 rpmg and 4 °C to collect the supernatant. The protein

concentration of each sample was measured using the BCA protein assay method.

##### SDS-PAGE electrophoresis

The 10 µg proteins of each sample were acquired and separated by 12% SDS-PAGE gel. Then, the separation gel was stained with Coomassie brilliant blue. Finally, the stained gel was scanned by an automatic digital gel image analysis system (Tanon 1600, China).

##### Protein digestion in solution

Take 50 µg protein from each sample, and dilute different groups of samples to the same concentration and volume. Add 25 mM DTT of the corresponding volume into the above protein solution to make the DTT final concentration about 5 mM, and incubate at 55 °C for 30 min. Then add the corresponding volume of iodoacetamide so that the final concentration is about 9 mM, and place in the dark for 15 min at room temperature. Then 6 times the volume of precooled acetone in the above system to precipitate the protein, and place it at –20 °C for overnight. After precipitation, the samples were centrifuged at 8000g for 10 min at 4 °C to collect the precipitate. Add the corresponding volume of trypsin (protein: enzyme = 50:1 (m/m)) to redissolve the protein precipitate, then the solutions were incubated for digestion at 37 °C for 12 h. Finally, the samples were lyophilized or evaporated after enzymolysis.

##### Peptide labeling and desalting

Each sample was mixed with the internal standard (iRT, Biognosys, ThermoFisher) at a volume ratio of 1:10, then the peptides were subjected to desalting using SOLA<sup>™</sup> SPE plates (ThermoFisher, 60,309–001).

##### Proteomic data acquisition

After desalting, peptides were separated on an 1100 HPLC System (Agilent) using an Agilent Zorbax Extend reversed-phase column (5 µm, 150 mm × 2.1 mm) at a flow rate of 250 µl/min and gradient elution was performed according to the following method [preparation of phase A (ACN-H<sub>2</sub>O (2: 98, v/v) and phase B (ACN-H<sub>2</sub>O (90: 10, v/v))]: 0 ~ 10 min, 2% B; 10 ~ 10.01 min, 2–5% B; 10.01–37 min, 5–20% B; 37–48 min, 20–40% B; 48–48.01 min, 40–90% B; 48.01–58 min, 90% B; 58–58.01 min, 90–2% B; 58.01–63 min, 2% B.

All analyses were performed by a Q-Exactive HF mass spectrometer (Thermo, USA) equipped with a Nanospray Flex source (Thermo, USA). Samples were loaded and separated by a C18 column (50 cm × 75 µm) on an EASY-nLC<sup>™</sup> 1200 system (Thermo, USA). The

flow rate was 300 nL/min and linear gradient was 90 min (0~60 min, 8–25% B; 60~79 min, 25–45% B; 79~80 min, 45–100% B; 80~90 min, 100% B; mobile phase A = 0.1% FA in water and B = 0.1% FA in 80%ACN).

For DDA parameters, the full MS scans were acquired in the mass range of 350–1650 m/z with a mass resolution of 120,000 and the automatic gain control (AGC) target value was set at  $3 \times 10^6$ . The 20 most intense peaks in MS were fragmented with higher-energy collisional dissociation (HCD) with a collision energy of 27. MS/MS spectra were obtained with a resolution of 30,000 with an AGC target of  $2 \times 10^5$  and a max injection time of 80 ms. The Q Exactive HF dynamic exclusion was set for 40.0 s and run under positive mode.

For DIA parameters, the full MS scans were acquired in the mass range of 350–1250 m/z with a mass resolution of 120,000 and the AGC target value was set at  $3 \times 10^6$ . The 32 acquisition windows in MS were fragmented with HCD with a collision energy of 28, and each acquisition window has 26 m/z. MS/MS spectra were obtained with a resolution of 30,000 with an AGC target of  $1 \times 10^6$ , and the maximum injection time was set to auto and run under positive mode.

#### **Data analysis**

DIA data were analyzed with Spectronaut Pulsar (Biognosys) against the uniprot-reviewed-Homo sapiens-20200817 database. Database search was performed with Trypsin digestion specificity. Alkylation on cysteine was considered a fixed modification in the database search. Protein, peptide and PSM's false discovery rate (FDR) all set to 0.01. For DIA data, the quantification FDR also set to 0.05. Quantity MS-level was set at MS2.

Protein areas were normalized, and principal component analysis (PCA) and t-tests were performed between HDLs from ARDS patients and healthy controls. Differentially expressed proteins (DEPs) were considered based on a fold-change of  $\geq 1.2$  or  $\leq 0.83$  and  $p < 0.05$ . Next, DEPs were annotated based on the Gene Ontology Consortium (GO), including cellular components, biological processes, and molecular functions.

#### **Targeted proteomics**

We used isotope-dilution parallel reaction monitoring (PRM) to quantify HDL proteins. Briefly, LC-MS/MS analyses were performed using an EASY-nLC™ 1200 UHPLC system (Thermo Fisher) coupled with a Q Exactive series mass spectrometer (Thermo Fisher).

#### **LC-MS/MS analysis pre-experiment**

A multistep gradient of 0.1% formic acid in water (solvent A) and 0.1% formic acid in acetonitrile (solvent B)

was used for the separation. HDL peptides mixture (1  $\mu$ g) were injected into a home-made C18 Nano-Trap column (2 cm  $\times$  75  $\mu$ m, 3  $\mu$ m) and peptides were separated on a home-made analytical column (15 cm  $\times$  150  $\mu$ m, 1.9  $\mu$ m). The separated peptides were analyzed by Q Exactive series mass spectrometer, with an ion source of Nano-spray Flex™ (ESI), spray voltage of 2.4 kV, and ion transport capillary temperature of 320 °C.

Full scan range from m/z 350 to 1500 with a resolution of 60,000 (at m/z 200), an AGC target value is  $3 \times 10^6$ , and a maximum ion injection time is 20 ms. The top 20 (40) precursors of the highest abundant in the full scan were selected and fragmented by HCD and analyzed in MS/MS, where the resolution is 15,000 (at m/z 200), the AGC target value is  $5 \times 10^4$ , the maximum ion injection time is 45 ms, a normalized collision energy of 27%, an intensity threshold of  $2.2 \times 10^4$ , and the dynamic exclusion parameter of 20 s. Raw data was searched using PD2.2 software with “missed cleavage” set to 0, and 1–3 unique peptides were selected for each protein.

After selecting the peptides, the information of the target peptide, such as m/z, charge number, and charge type, was input into the “inclusion list”. The mixed peptides described above were analyzed by “full scan” followed by “PRM” pattern. The chromatographic separation and full scan condition are the same as above. The PRM was set as the resolution of 30,000 (at 200 m/z) with an AGC target value of  $5 \times 10^4$ , a maximum ion injection time of 80 ms, a normalized collision energy of 27%. The off-line data was analyzed by Skyline software to determine whether the selected peptides were usable based on reproducibility and stability.

#### **LC-MS/MS analysis**

The same amount of trypsin treated-peptide of each sample was taken and spiked with an equal amount of the labeled peptide DSPSAPVNVTVR (red bold V for heavy isotope labeling) as an internal standard. Samples were analyzed using a “full scan” followed by a “PRM” pattern, as described above. The off-line data was analyzed by Skyline software, and the peak area was corrected using the internal standard peptide.

Based on the DIA-MS proteome analysis results, we selected 18 HDL proteins with the most significant fold changes for relative quantification. Peptides monitored for each protein by PRM analysis were shown in Supplemental Table 1.

#### **Construction of Pro-SFTPB enriched HDL**

HDL (1 mg/ml, 250  $\mu$ g, Sigma, L1567) was incubated with 16.5  $\mu$ g recombinant human SFTPB (0.066 mg/ml, Sino Biological, 17,682-H08C1) in PBS containing 10 mM of reduced glutathione at 37 °C for 2 h. Then,

the mixture was reisolated with ultrafiltration tubes to remove free SFTPb. Immunoblotting of SFTPb showed HDL successfully carried SFTPb (Santa Cruz, sc-13978).

### Cell culture and differentiation

The THP1 cell line was obtained from ATCC, and cultured in RPMI 1640 medium supplemented with 10% FCS and 2 mmol/L L-glutamine. THP1 cells were differentiated using 100 µg/ml phorbol myristate acetate (PMA, Sigma) for 48 h. Differentiation of PMA-treated cells was enhanced after the initial 48 h stimulus by removing the PMA-containing media and then incubating the cells in fresh RPMI 1640 for 24 h.

### Phagocytotic assay and intracellular ROS detection

The phagocytic activity of macrophages was assessed by quantifying the uptake of red fluorescent pHrodo bioparticles (Invitrogen, #P35360, USA). The THP1 cells were plated into 24-well plates at a density of 10,000 cells per well and then differentiated into macrophages. A suspension of *E. coli* particles was added to the cell culture microplate at a dilution of 1:20. The cell-particle mixture was then incubated for 30 min at 37 °C to evaluate the uptake activity using fluorescence microscopy.

Intracellular oxidative stress was assessed by detecting the generation of ROS using the fluorescent probe DCFH-DA (Beyotime, #S0033S, China). 30 min after HDL exposure, the Thp1-derived M0 cells were treated with 10 µM/mL DCFH-DA and incubated for 30 min at 37 °C, avoiding light. Fluorescence intensity was measured with a Varioskan Flash microplate reader (ThermoFisher Scientific Inc., USA) with excitation at 488 nm and emission at 525 nm.

### Quantitative real-time PCR

Total RNA was extracted using Trizol (Invitrogen, 15,596,018) according to the manufacturer's manual and the cDNA was synthesized using PrimeSTAR® Max DNA Polymerase (Takara, R045A). qPCR assay was performed using TB Green® Premix Ex Taq™ II (Takara, RR820) and the data were normalized to the GAPDH content and analyzed by the  $2^{-\Delta\Delta Ct}$  method relative to control groups. The primers used in qPCR are shown in the table below.

TNF-α	F	CCTCTCTAATCAGCCCTCTG
	R	GAGGACCTGGGAGTAGATGAG
IL-1β	F	ATGATGGCTTATTACAGTGGCAA
	R	GTCGGAGATTCTAGCTGGA

IL-8	F	ACTGAGAGTGATTGAGAGTGGAC
	R	AACCCTCTGCACCCAGTTTTTC
MRC-1	F	GGGTTGCTACTACTCTCTATGC
	R	TTTCTTGCTCTGTTGCCGTAGTT
GAPDH	F	GAAGGTGAAGTCCGGAGTC
	R	GAAGATGGTGATGGGATTTTC

### Statistical analysis

Categorical variables are presented as numbers and percentages. Continuous data are expressed as mean ± SEM (standard error of the mean) for normally distributed variables, and medians (25th~75th percentiles) for non-normally distributed variables. Statistical comparisons between two groups were performed using the chi-squared test or Fisher's exact test for categorical variables, the Mann-Whitney U test for non-normally distributed continuous variables, and the two-tailed Student's t-test for normally distributed continuous variables. For the comparisons of three groups, the one-way ANOVA followed by a post hoc test was applied. Pearson correlation analysis was used to assess the correlation of pro-SFTPb with a panel of 38 cytokines and other HDL protein components. The simple linear regression was further used to test whether pro-SFTPb in HDL could capture effects on the SAA2 and PON3 contents. Furthermore, receiver operating characteristic (ROC) curves were depicted, and the area under the curves [AUC, with 95% confidence intervals (CIs)] were calculated to evaluate the value of pro-SFTPb level in HDL and SOFA score for the prediction of the 28-day mortality. A two-sided  $p < 0.05$  was considered statistically significant, and data were analyzed using the SPSS software package (version 19.0, SPSS, Chicago, IL, USA).

### Results

#### The change in the HDL protein profile was associated with the functional transition of HDL in ARDS patients

To examine HDL protein component changes in ARDS patients, a discovery cohort of 8 individuals with ARDS and an equal number of age- and sex-matched 8 healthy controls (HCs) were enrolled. The baseline clinical data of HCs and ARDS patients are presented in Table 1. Compared with the HC group, ARDS patients exhibited significantly reduced HDL-C levels ( $p = 0.001$ ). Their plasma samples were collected, and plasma pooled from 2 subjects with similar ages and clinical situations was used for the HDL isolation procedure to improve efficiency and capacity in following proteomics analyses.

The M0 macrophages (unpolarized resting state) differentiated from human monocyte THP1 cells were used to assess the influence of HDLs on M1 polarization. The treatment of phorbol myristate acetate (PMA) for 48 h

**Table 1** Characteristics of patients with septic ARDS and healthy subjects in discovery cohort

Variables	Healthy subjects (n = 8)	ARDS patients (n = 8)	p
Male, n (%)	4 (50.0)	4 (50.0)	> 0.990
Age (years)	62 (60~64)	64 (61~65)	0.505
BMI(kg/m <sup>2</sup> )	22.37 ± 0.27	23.08 ± 0.47	0.209
Current smoker, n (%)	3 (37.5)	4 (50.0)	> 0.990
Etiology, n (%)	N/A		
Pneumonia		6 (75.0)	
Abdominal infection		2 (25.0)	
Underlying diseases, n (%)	N/A		
Hypertension		2 (25.0)	
APACHE II score at admission	N/A	18 ± 3	
SOFA score at admission	N/A	9 ± 1	
White blood cell (× 10 <sup>9</sup> /L)	6.44 (5.95~7.62)	9.85 (5.44~13.73)	0.105
C-reactive protein (mg/L)	N/A	101 ± 13	
Procalcitonin (ng/ml)	N/A	5.47 (1.79~14.88)	
PaO <sub>2</sub> /FiO <sub>2</sub> , n (%)	N/A		
200–300		2 (25.0)	
100–200		3 (37.5)	
≤ 100		3 (37.5)	
HDL-C (mmol/l)	1.49 ± 0.11	0.83 ± 0.10	<b>0.001</b>
Complications, n (%)	N/A		
Liver dysfunction		5 (62.5)	
Acute kidney injury		4 (50.0)	
28-day mortality, n (%)	N/A	3 (37.5)	

BMI: body mass index, APACHE II: acute physiology and chronic health evaluation II, SOFA: sequential organ failure assessment, PaO<sub>2</sub>: arterial oxygen tension, FiO<sub>2</sub>: fraction of inspired oxygen, HDL-C: high density lipoprotein-cholesterol

induced the differentiation of THP-1 monocytes in suspension into adherent M0 macrophages with round and slightly elongated cell morphology (Supplemental Figure 2). The HDL from ARDS patients (A-HDL) markedly enhanced M1 marker gene expression compared to HDL from normal subjects (N-HDL), accompanied by M1-like morphological changes, including larger and irregular cell shapes (Fig. 1A, Supplemental Figure 2). These observations suggested a pro-inflammatory transition of A-HDL. In order to identify the key protein components associated with the adverse transition in A-HDL, we designed a series of experiments, including proteomic analysis on the discovery cohort, targeting protein MS quantification on the validation cohort, and in vitro confirmation (Fig. 1B).

First, the HDLs from the discovery cohort were further subjected to DIA-MS proteomic analyses. 384 distinct proteins were identified based on the analysis of 3,482 peptides. The following PCA results revealed good sample specificity (Fig. 2A). Furthermore, a comparative analysis identified 102 differentially expressed proteins (DEPs) between A-HDL and N-HDL with 53 upregulated and 49 downregulated (Fig. 2B, C). The GO analysis on

these DEPs showed the most affected processes involved in HDL particles, acute phase response, platelet degranulation, regulation of the immune system process, and antioxidant activity (Fig. 2D). The remodeling of protein components in A-HDL was consistent with the pro-inflammatory transition.

#### Confirmation of A-HDL protein component changes in a validation cohort and association of these changes with prognosis of ARDS

To validate the protein component changes in A-HDL identified by proteomic analysis, we enrolled a validation cohort including 22 ARDS patients (12 survivors and 10 non-survivors) and 10 healthy controls (Fig. 3A, a flow-chart of subject enrollment). The baseline clinical data of healthy individuals and ARDS patients are presented in Table 2. Consistent with the discovery cohort, ARDS patients in the validation cohort exhibited a statistically significant decrease in HDL-C levels ( $p=0.002$ ). There were no significant differences in HDL-C levels between survivors and non-survivors.

Using targeted proteomics analysis, 18 HDL proteins with the most significant fold-changes in previously

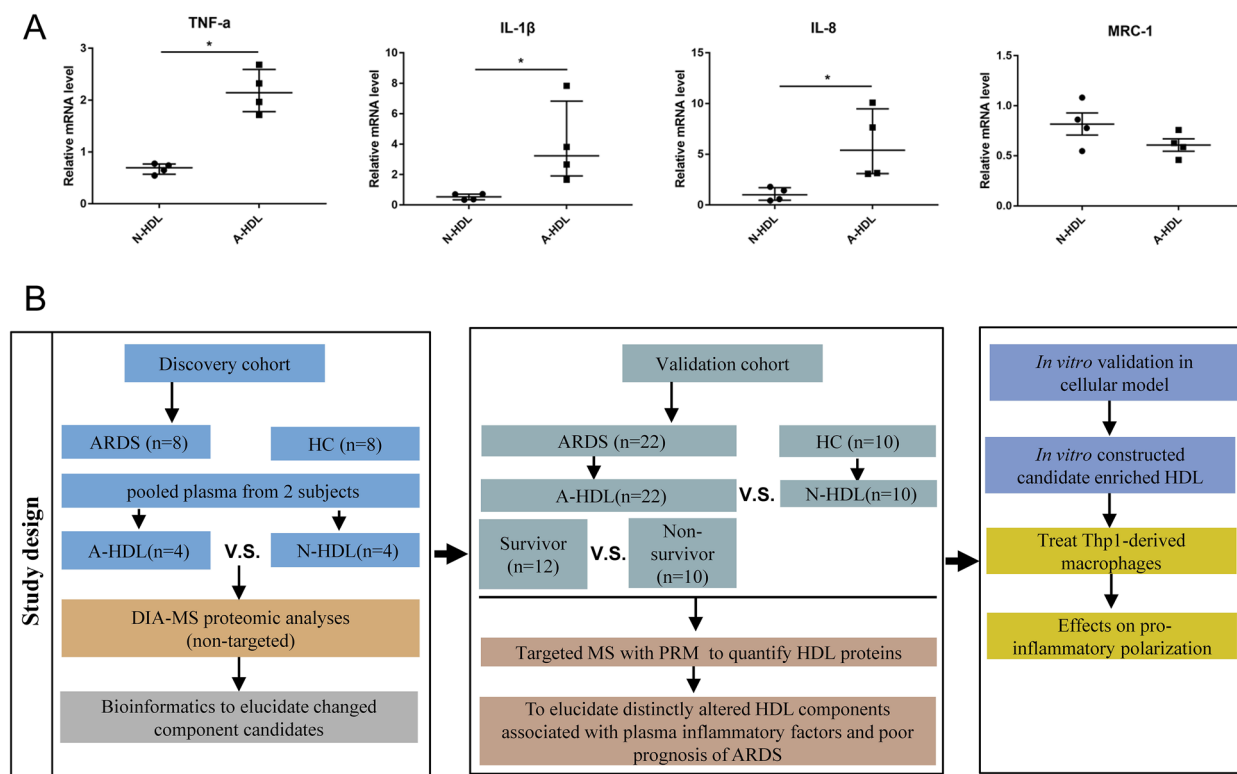


**Fig. 1** The HDL from ARDS patients indicated an adverse functional transition. **A** The A-HDL treatment (50 µg/ml, 12 h) induced M1 polarization of THP1-derived macrophage by qPCR assay of M1/M2-associated markers (n=4 per group). \*p < 0.05; M1 marker: TNF-α, IL-1β and IL-8; M2 marker: MRC-1. **B** The study design encompassed a series of experiments including proteomic analysis on the discovery cohort, targeting protein MS quantification on the validation cohort, and subsequent in vitro confirmation. ARDS, acute respiratory distress syndrome; HDL, high-density lipoprotein; N-HDL, HDL from normal subjects; A-HDL, HDL from ARDS patients; TNF, tumor necrosis factor; IL-, interleukin-; MRC-1, mannose receptor C-type 1; HC, healthy controls; DIA-MS, data-independent acquisition mass spectrometry

identified 102 DEPs were further quantified in HDL from the validation cohort by PRM, in which 12 HDL-proteins were significantly changed in A-HDL versus N-HDL (Supplemental Table 1). The contents of pro-SFTPb, apoE, LBP, SAA1 and SAA2 in A-HDL were markedly increased, whereas the contents of apoM, apo-II, apo-IV, PON1, PON3, SERPINA5 and IGFBP3 were significantly decreased compared to N-HDL (Fig. 3B).

To further explore whether these changed HDL-protein contents are associated with the prognosis of ARDS, we compared these proteins between survivors and non-survivors. Interestingly, among these proteins, only the pro-SFTPb component showed significantly higher in non-survivor patients than in survivors (Fig. 4A). Furthermore, the ROC curves for pro-SFTPb in HDL and SOFA score were plotted to compare the predictive accuracy and specificity for 28-day mortality (Fig. 4B). The area under the curves for HDL-pro-SFTPb and SOFA score were 0.783 (p=0.025, 95% CI 0.589–0.978) and 0.725 (p=0.075, 95% CI 0.511–0.939), suggesting a favorable prediction value of HDL-pro-SFTPb for 28-day

mortality in ARDS patients. These intriguing findings focus our attention on the HDL-pro-SFTPb content change, which likely has a critical role in adverse HDL transition leading to poor progression of ARDS.

**The correlation of HDL-pro-SFTPb content with plasma levels of inflammatory factors**

To further confirm the significance of HDL-pro-SFTPb, we examined the correlation of HDL-pro-SFTPb content with plasma levels of 38 inflammatory factors linked to acute respiratory diseases, including cytokines, chemokines, and growth factors. Pearson’s correlation coefficients are shown in Table 3. HDL-Pro-SFTPb levels exhibited a statistically significant positive correlation with cytokines such as IL-3 (r=0.380, p=0.032), IL-8 (r=0.439, p=0.012), IL-15 (r=0.404, p=0.022), IL-18 (r=0.464, p=0.007), IP-10 (r=0.497, p=0.004), MCP-1 (r=0.355, p=0.046), MCP-3 (r=0.385, p=0.029) and MIG (r=0.527, p=0.002), while presented a statistically significant negative correlation with MDC (r=-0.403, p=0.022) and

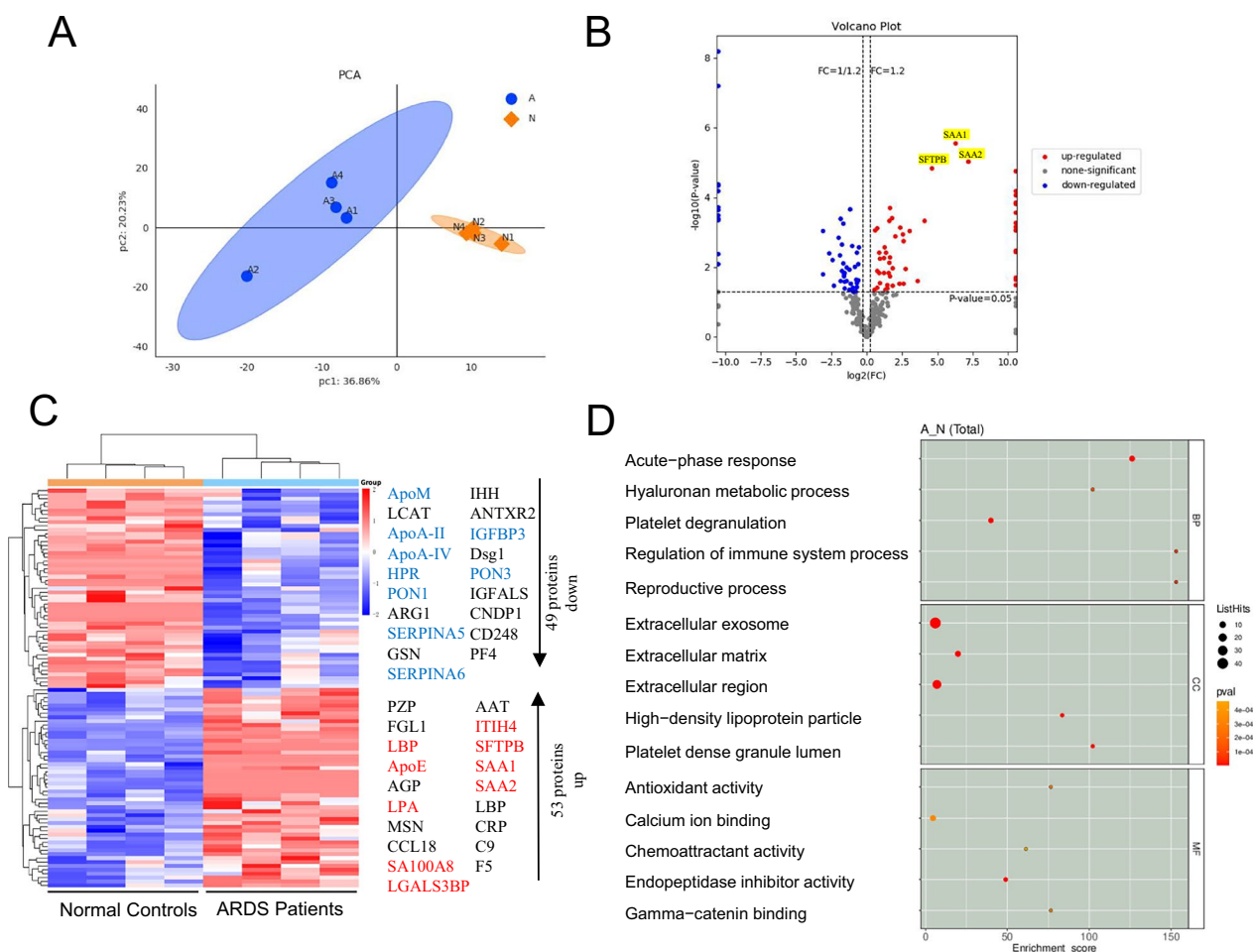


**Fig. 2** The pro-inflammatory HDL from ARDS patients showed marked changes in protein profile by proteomic analysis. The plasma samples from 8 ARDS patients and 8 healthy controls were collected. The plasma mixture from 2 subjects with similar ages and clinical situations was used for the isolation procedure to improve the quality. **A** The DEPs between N-HDL and A-HDL by DIA-MS proteome analysis. There was significant specificity between N-HDL and A-HDL by PCA. **B, C** The volcano plot and heatmap showed that a total of 384 proteins were identified with 53 upregulated and 49 downregulated proteins between A-HDL and N-HDL. The blue and red-colored proteins denoted the 18 HDL proteins with the most significant fold-changes. **D** The Gene Ontology analysis on these DEPs and the most affected processes were presented. ARDS, acute respiratory distress syndrome; HDL, high-density lipoprotein; N-HDL, HDL from normal subjects; A-HDL, HDL from ARDS patients; DEPs, differentially expressed proteins; DIA-MS, data-independent acquisition mass spectrometry; PCA, principal component analysis; SFTPB, pulmonary surfactant-associated protein B; SAA, serum amyloid A; Apo, apolipoprotein; HPR, haptoglobin-related protein; PON, paraoxonase; SERPIN, serpin family A member; IGFBP3, insulin-like growth factor-binding protein 3; LBP, lipopolysaccharide-binding protein; LPA, apolipoprotein(a); SA100A8, S100 calcium-binding protein A8; LGALS3BP, lectin, galactoside-binding, soluble 3 binding protein; ITIH4, inter-alpha-trypsin inhibitor 4

platelet-derived growth factor (PDGF)-AA ( $r = -0.370$ ,  $p = 0.037$ ). These findings depicted a clear positive correlation of HDL-pro-SFTPB content with systemic inflammation, which was potentially involved in the development of septic-ARDS.

**The correlation of pro-SFTPB content with other significantly changed HDL proteins**

The altered HDL protein components validated by targeted proteomics are involved in the regulation of various HDL functions, including HDL particle components

(apolipoproteins), pro-inflammatory substances (SAAs) and anti-oxidative proteins (PONs). The correlations between the contents of pro-SFTPB and these proteins in A-HDL were examined (Table 4). As expected, there was a statistically positive correlation between pro-SFTPB with SAA2 in HDL ( $r = 0.350$ ,  $p = 0.049$ ), whereas a statistically negative correlation between pro-SFTPB with PON3 in HDL ( $r = -0.508$ ,  $p = 0.003$ ). We further performed a linear regression assay to test whether pro-SFTPB content could capture effects on the SAA2 and PON3 contents. Of note, the linear regression assay also

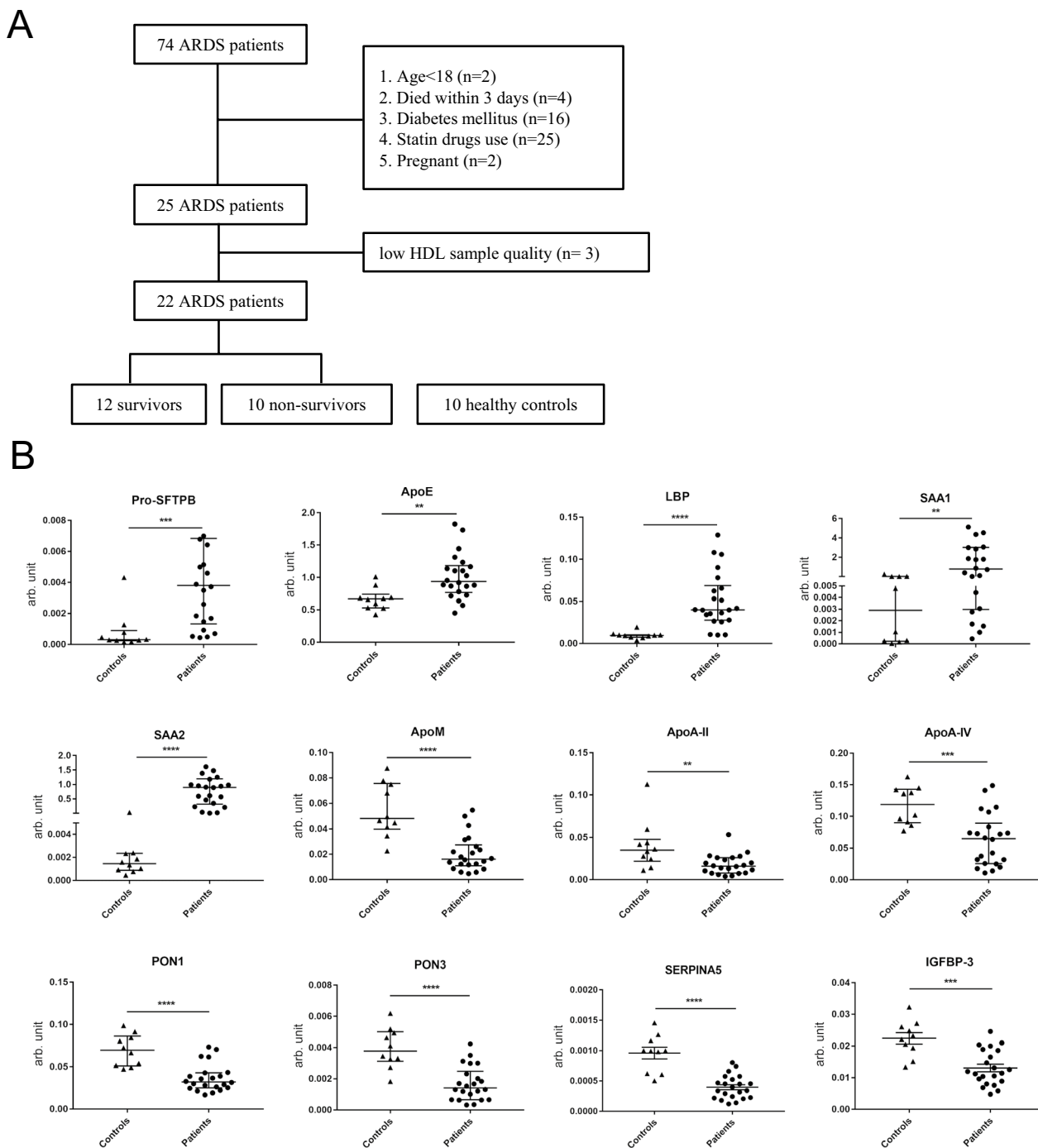


**Fig. 3** The altered HDL proteins identified in the discovery cohort were confirmed in the validation cohort. **A** Flowchart of ARDS patient enrollment along with healthy controls. **B** The significantly changed HDL constituent proteins in A-HDL versus N-HDL in the validation cohort. ARDS, acute respiratory distress syndrome; HDL, high-density lipoprotein; N-HDL, HDL from normal subjects; A-HDL, HDL from ARDS patients; pro-SFTPB, pro-pulmonary surfactant-associated protein B; Apo, apolipoprotein; SAA, serum amyloid A; PON, paraoxonase; LBP, lipopolysaccharide binding protein; SERPINA5, serpin family A member 5; LGALS3BP, lectin galactoside-binding soluble 3 binding protein; \*\* $p < 0.01$ ; \*\*\* $p < 0.001$ ; \*\*\*\* $p < 0.0001$

showed that pro-SFTPB in HDL could capture the positive effect on the pro-inflammatory component SAA2 and the negative effect on the anti-oxidative protein

PON3 (Fig. 5). These results suggest that the increase in pro-SFTPB content could be one of the triggers for adverse HDL transition.

**Table 2** Characteristics of patients with septic ARDS and healthy subjects in validation cohort

Variables	Healthy subjects (n = 10)	ARDS patients (n = 22)	p	Survivors (n = 12)	Nonsurvivors (n = 10)	p
Male, n (%)	6 (60.0)	15 (68.2)	0.703	8 (66.7)	7 (70.0)	> 0.990
Age (years)	64 (63~69)	70 (55~81)	0.483	64 (54~81)	71 (66~82)	0.456
BMI(kg/m <sup>2</sup> )	23.69±0.79	23.95±0.81	0.845	24.53±1.06	23.26±1.27	0.447
Current smoker, n (%)	4 (40.0)	12 (54.5)	0.704	6 (50.0)	6 (60.0)	0.691
Etiology, n (%)	N/A					
Pneumonia		14 (63.6)		8 (66.7)	6 (60.0)	> 0.990
Abdominal infection		8 (36.4)		4 (33.3)	4 (40.0)	
Underlying diseases, n (%)	N/A					
Hypertension		10 (45.5)		5 (41.7)	5 (50.0)	> 0.990
APACHE II score at admission	N/A	21 (11~29)		17±3	24±3	0.076
SOFA score at admission	N/A	9±1		8±1	11±1	<b>0.046</b>
Laboratory data at admission						
White blood cell (×10 <sup>9</sup> /L)	N/A	12.7±1.2		11.0 (8.8~14.6)	12.8 (7.2~20.0)	0.722
Neutrophil granulocyte (×10 <sup>9</sup> /L)	N/A	11.1±1.2		10.0 (8.1~12.3)	10.0 (6.7~18.7)	0.454
Haemoglobin (g/L)	N/A	104±5		107±7	100±7	0.483
Platelet (×10 <sup>9</sup> /L)	N/A	162±21		194 (77~269)	144 (94~176)	0.381
C-reactive protein (mg/L)	N/A	110.1 (73.2~121.8)		85.2±16.3	136.4±23.1	0.078
Procalcitonin (ng/ml)	N/A	5.7 (0.3~10.7)		8.3 (0.2~10.8)	4.0 (0.5~19.0)	0.923
PH	N/A	7.43±0.02		7.43±0.02	7.42±0.03	0.866
PaCO <sub>2</sub> (mmHg)	N/A	35.5 (28.0~45.3)		35.5 (28.0~49.8)	34.0 (29.0~41.8)	0.722
PaO <sub>2</sub> /FiO <sub>2</sub> , n (%)	N/A					0.636
200–300		6 (27.3)		4 (33.3)	2 (20.0)	
100–200		10 (45.5)		6 (50.0)	4 (40.0)	
≤ 100		6 (27.3)		2 (16.7)	4 (40.0)	
Lactate (mmol/L)	N/A	1.7 (1.2~2.8)		1.69±0.26	2.73±0.58	0.098
HDL-C (mmol/l)	1.50±0.11	0.94±0.10	<b>0.002</b>	0.90 (0.80~1.23)	0.83 (0.40~1.09)	0.254
TBIL (umol/L)	N/A	15.00 (10.43~32.75)		12.85 (8.13~60.20)	16.90 (13.83~32.75)	0.314
Creatinine (umol/L)	N/A	123.0 (49.3~204.9)		96.1 (47.0~159.6)	159.3 (49.3~305.0)	0.228
Complications, n (%)	N/A					
Liver dysfunction		7 (31.8)		4 (33.3)	3 (30.0)	> 0.990
Acute kidney injury		6 (27.3)		2 (16.7)	4 (40.0)	0.348
Treatment during RICU, n (%)	N/A					
Vasopressors		17 (77.3)		8 (66.7)	9 (90.0)	0.323
CRRT		4 (18.2)		1 (8.3)	3 (30.0)	0.293
Invasive mechanical ventilation		22 (100.0)				0.646
Pressure controlled ventilation		16 (72.7)		8 (66.7)	8 (80.0)	
Volume controlled ventilation		6 (27.3)		4 (33.3)	2 (20.0)	
RICU days	N/A	12 (8~17)		11 (8~17)	12 (7~16)	0.582

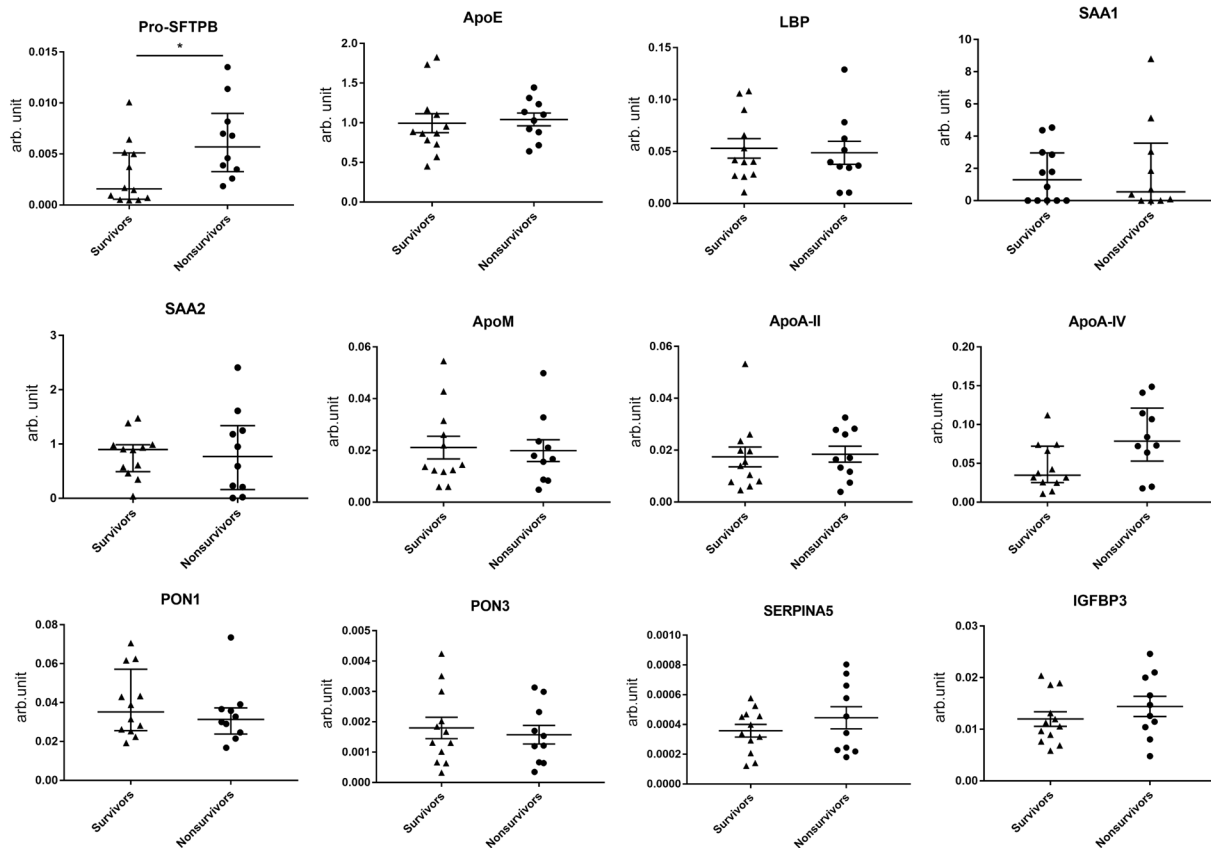
BMI: body mass index, APACHE II: acute physiology and chronic health evaluation II, SOFA: sequential organ failure assessment, PaCO<sub>2</sub>: arterial carbon dioxide tension, PaO<sub>2</sub>: arterial oxygen tension, FiO<sub>2</sub>: fraction of inspired oxygen, HDL-C: high density lipoprotein-cholesterol, TBIL: total bilirubin, CRRT: continuous renal replacement therapy, RICU: respiratory intensive care unit. Bold value indicates statistical significance

### The enrichment of pro-SFTPb within the HDL promoted M1 macrophage polarization in vitro

The clinically relevant evidence showed a critical role of increased pro-SFTPb content in adverse HDL transition. To provide direct evidence for its role in the pro-inflammatory transition of HDL, we in vitro constructed

pro-SFTPb enriched HDL by using normal HDL and recombinant pro-SFTPb and examined the effect on M1 polarization of THP1-derived M0 macrophage (Fig. 6A). The immunoblot of SP-B using native-PAGE showed the shift of the pro-SFTPb band from ~42KD to ~200KD, suggesting that pro-SFTPb was successfully incorporated

**A**



**B**

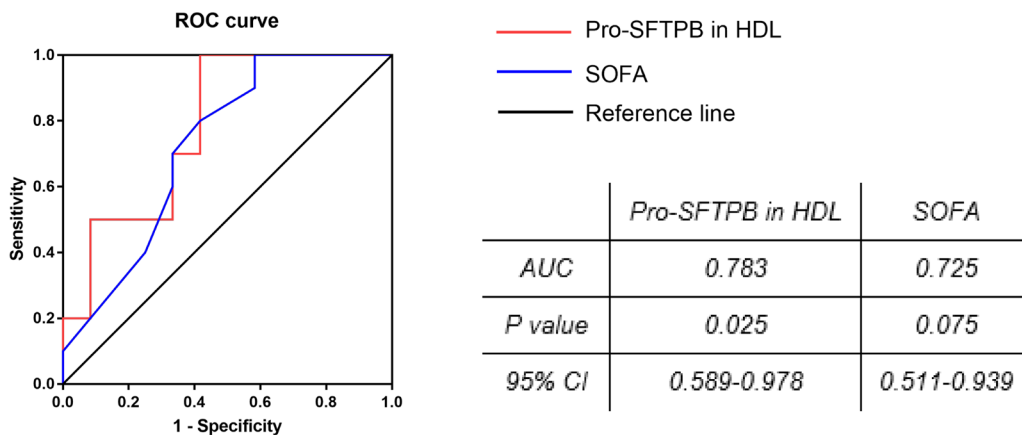


**Fig. 4** Pro-SFTPb in HDL is associated with the prognosis of ARDS patients. **A** Only pro-SFTPb in HDL showed a significant difference between survivors (n = 12) and non-survivors (n = 10). **B** ROC curves for pro-SFTPb in HDL and SOFA score in prediction of the 28-day mortality in ARDS patients. ARDS, acute respiratory distress syndrome; HDL, high density lipoprotein; Pro-SFTPb, pro-pulmonary surfactant-associated protein B; Apo, apolipoprotein; SAA, serum amyloid A; PON, paraoxonase; LBP, lipopolysaccharide binding protein; SERPINA5, serpin family A member 5; LGALS3BP, lectin galactoside-binding soluble 3 binding protein; ROC, receiver operating characteristic; AUC, area under the curve; CI, confidence interval; SOFA, sequential organ failure assessment; \*p < 0.05

into HDL particles (Fig. 6B). We explored dose-dependent (50, 70 and 100 µg/ml) effects of pro-SFTPb enriched HDL (PS-HDL) on M1 macrophage polarization by the

expression of TNF-α and IL-8, the treatment at 50 mg/ml failed to induce macrophage activation and the treatment at 70 mg/ml partially induced macrophage activation

**Table 3** Correlation analysis between the HDL-pro-SFTPb level and cytokines

Cytokines	Pro-SFTPb	
	r	p
sCD40L	-0.052	0.776
G-CSF	0.010	0.955
GRO-α	0.341	0.056
IFN-α	0.293	0.104
IFN-γ	0.076	0.679
IL-1α	0.226	0.213
IL-1β	0.068	0.713
IL-1RA	0.028	0.881
IL-2	0.218	0.232
<b>IL-3</b>	<b>0.380</b>	<b>0.032</b>
IL-4	0.062	0.735
IL-5	0.123	0.503
IL-6	0.201	0.269
IL-7	0.125	0.494
<b>IL-8</b>	<b>0.439</b>	<b>0.012</b>
IL-9	0.133	0.467
IL-10	0.249	0.170
IL-13	0.037	0.841
<b>IL-15</b>	<b>0.404</b>	<b>0.022</b>
IL-17A	0.203	0.266
IL-17E	0.168	0.359
IL-17F	0.207	0.255
<b>IL-18</b>	<b>0.464</b>	<b>0.007</b>
IL-22	0.003	0.985
IL-27	0.061	0.738
<b>IP-10</b>	<b>0.497</b>	<b>0.004</b>
<b>MCP-1</b>	<b>0.355</b>	<b>0.046</b>
<b>MCP-3</b>	<b>0.385</b>	<b>0.029</b>
M-CSF	0.321	0.073
<b>MDC</b>	<b>-0.403</b>	<b>0.022</b>
<b>MIG</b>	<b>0.527</b>	<b>0.002</b>
MIP-1α	0.230	0.206
MIP-1β	0.038	0.837
<b>PDGF-AA</b>	<b>-0.370</b>	<b>0.037</b>
PDGF-BB	-0.341	0.056
TGF-α	0.261	0.150
TNF-α	0.180	0.323
TNF-β	-0.050	0.784

pro-SFTPb: pro-pulmonary surfactant-associated protein B, HDL: high density lipoprotein, sCD40L: soluble CD40 ligand, G-CSF: granulocyte colony-stimulating factor, GRO: growth-related oncogene, IFN-: interferon-, IL-: interleukin-, IP-10: interferon-inducible protein-10, MCP: monocyte chemotactic protein, M-CSF: macrophage colony-stimulating factor, MDC: macrophage-derived chemokine, MIG: monokine induced by interferon-γ, MIP-: macrophage inflammatory protein-, PDGF-: platelet-derived growth factor-, TGF: transforming growth factor, TNF: tumor necrosis factor. Bold value indicates statistical significance

**Table 4** Correlation analysis between the pro-SFTPb levels in HDL and other HDL proteins

Proteins	Pro-SFTPb	
	r	p
ApoE	0.120	0.514
ApoM	-0.305	0.089
ApoA2	-0.339	0.058
ApoA4	-0.228	0.209
HPR	-0.093	0.612
PON1	-0.256	0.157
<b>PON3</b>	<b>-0.508</b>	<b>0.003</b>
SERPINA5	-0.242	0.182
SERPINA6	-0.008	0.966
IGFBP3	-0.229	0.207
LBP	0.182	0.319
LPA	-0.247	0.173
S100A8	-0.288	0.111
LGALS3BP	0.311	0.083
ITIH4	0.225	0.215
SAA1	0.112	0.541
<b>SAA2</b>	<b>0.350</b>	<b>0.049</b>

pro-SFTPb: pro-pulmonary surfactant-associated protein B, HDL: high density lipoprotein, Apo: apolipoprotein, HPR: haptoglobin related protein, PON: paraoxonase, SERPINA: serpin family A member, IGFBP3: insulin-like growth factor binding protein 3, LBP: lipopolysaccharide binding protein, LPA: lysophosphatidic acid, LGALS3BP: lectin galactoside-binding soluble 3 binding protein, ITIH4: inter-alpha-trypsin inhibitor heavy chain H4, SAA: serum amyloid A. Bold value indicates statistical significance

(Supplemental Figure 3). The PS-HDL (100ug/ml) significantly promoted M1 polarization, as indicated by marked upregulations of M1-associated markers (TNF-α, IL-1β, IL-8), but not the M2-associated marker (mannose receptor C-type 1, MRC1) (Fig. 6C). In addition, the capability of macrophages to engulf and eliminate microorganisms (M1 polarization characteristics) was evaluated by quantifying the uptake of labeled E. coli particles. Consistently, the macrophages treated by PS-HDL exhibited a significant increase in the number of ingested particles compared to HDL treatment (Fig. 6D). Moreover, macrophages exposed to PS-HDL demonstrated a notably higher production of ROS than those treated with HDL (Fig. 6E). Although pro-SFTPb is nearly entirely bound to HDL in plasma [22], we exposed M0 macrophages with free recombinant pro-SFTPb protein (60 ng/ml and 90 ng/ml) to assess its potential impacts independent of HDL particles. As expected, pro-SFTPb treatment failed to induce M1 polarization, suggesting that HDL with pro-SFTPb incorporation accounted for the pro-inflammatory effects rather than the pro-SFTPb itself (Supplemental Figure 4).

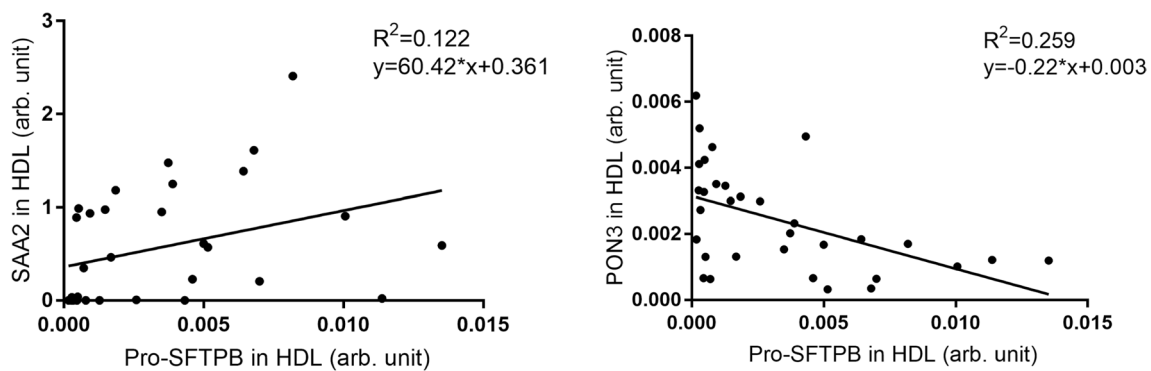


**Fig. 5** Scatter diagram for the relationship between pro-SFTPb and SAA2 and PON3 in HDL. pro-SFTPb, pro-pulmonary surfactant-associated protein B; SAA2, serum amyloid A-2 protein; PON3, serum paraoxonase 3; HDL, high density lipoprotein

## Discussion

Our present research identified a profile change of HDL protein components in septic-ARDS patients, in which 18 HDL proteins were confirmed in the validation cohort, involved in the regulation of various HDL functions, including HDL particle components, pro-inflammatory composition and anti-oxidative proteins. Among these proteins, increased HDL-pro-SFTPb was significantly associated with poor prognosis of ARDS patients. HDL-pro-SFTPb content was correlated with levels of plasma cytokines and chemokines, as well as with the pro-inflammatory component SAA2 and the anti-oxidative protein PON3. The *in vitro* results showed that pro-SFTPb enriched HDL markedly promotes M1 polarization. This clinical relevance and mechanistic studies indicate the importance of increased pro-SFTPb for HDL pro-inflammatory transition during ARDS, leading to exacerbated progression of septic-ARDS through enhancing M1 macrophage polarization. HDL-pro-SFTPb could be a potential prognostic biomarker for septic ARDS.

HDL is a heterogeneous particle containing lipids and distinct components of proteins involved in various biological functions. The different functional properties of HDL are weakly correlated with each other and determined by different structural components, especially the protein contents [16, 17, 20]. Increasing evidence indicates that HDL's adverse function transition is accompanied by composition modified upon inflammatory milieu [14, 18–20]. Herein, HDL from septic-ARDS patients also showed pro-inflammatory transition by significantly promoting M1 macrophage polarization, which was accompanied by significant protein profile changes, including an increase in corresponding pro-inflammatory components (SAA1/2) and a decrease in anti-oxidative proteins (PON1/3, apoA-II/IV, apoM). For the first time, our interesting findings depict a link between HDL

functionality and the remodeling of protein constituents during septic-ARDS. Our observations are consistent with recent studies on diseases characterized by acute and chronic inflammatory disorders. The levels of SAA1 and SAA2 in HDL have increased by over 50% in hospitalized COVID-19 patients, and apoM in HDL exhibits an inverse correlation with odds of death due to COVID-19 complications [19]. The levels of apoA-I, apoA-IV, and lactate dehydrogenase (LDH) in HDL were inversely associated with diabetes and atherosclerotic cardiovascular disease [20].

Among the HDL proteins changed in ARDS patients, the clinical relevance of pro-SFTPb to the prognosis of ARDS was highlighted. Increased pro-SFTPb in HDL was significantly inversely correlated with 28-day mortality, as indicated by the ROC curve with an AUC of 0.783 (considered as acceptable discrimination) and a p-value of 0.025. However, as a common index for the severity of ARDS, the SOFA score returns a non-significant p-value of 0.075 and an AUC of 0.725 for ROC assay in our cohort, which would be due to the limited sample size. HDL-pro-SFTPb component seems to have a better predictive ability for 28-day mortality than the SOFA score. Furthermore, in line with clinical relevance to poor prognosis, HDL-pro-SFTPb content is correlated with the plasma level of pro-inflammatory factors and HDL inflammatory components. These results further indicated that increased pro-SFTPb contributes to triggering the pro-inflammatory transition of HDL, leading to exacerbated progression of ARDS. Although previous studies of cardiovascular diseases have shown that pro-SFTPb enrichment diminishes the antioxidant capacity of HDL in patients with heart failure and HDL-pro-SFTPb content was inversely associated with diabetes and atherosclerosis [22, 23], our study, for the first time, provides evidence for its essential role in the

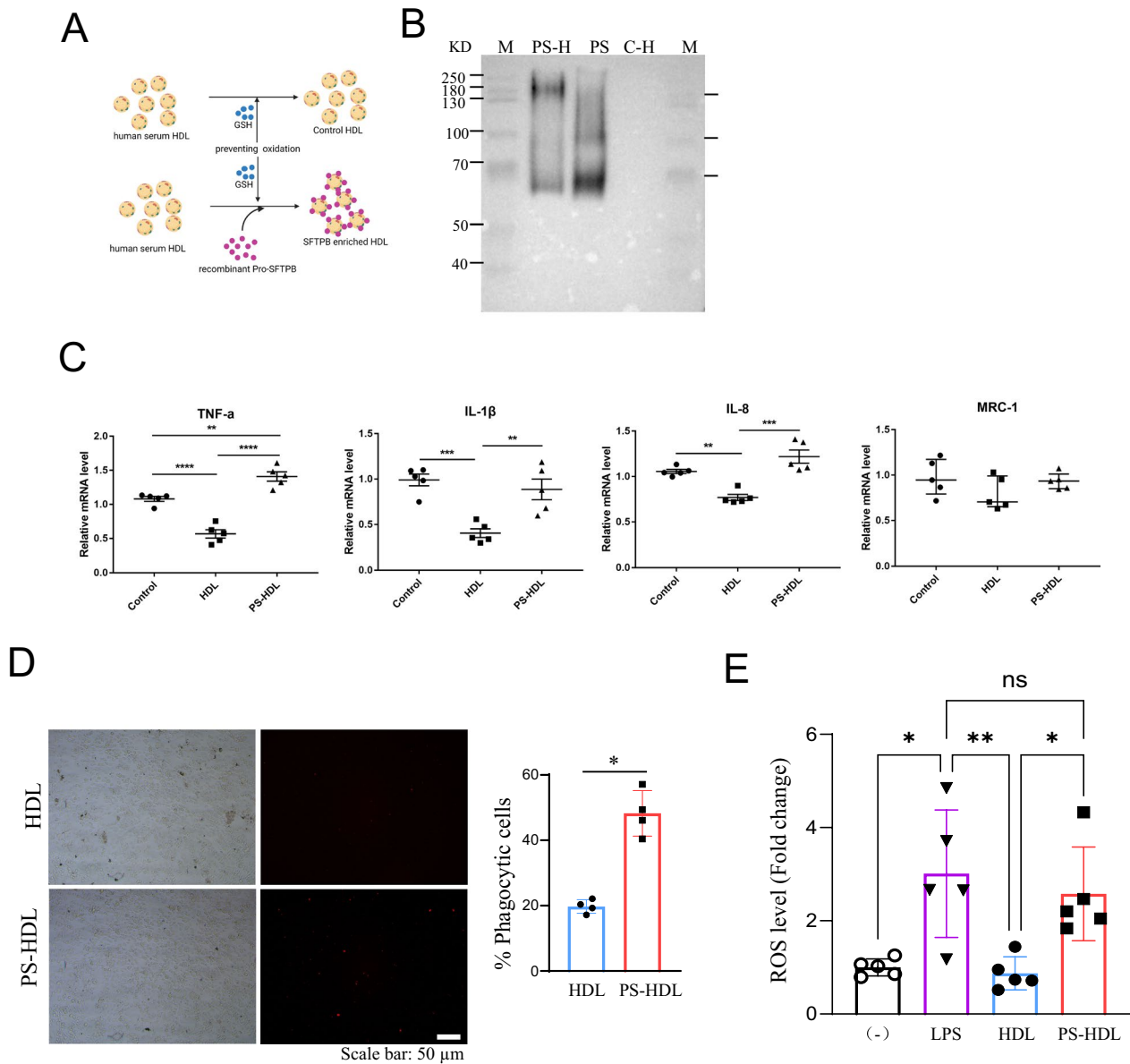


**Fig. 6** Pro-SFTPB enriched HDL induced M1 macrophage polarization. **A** Schematic diagram of HDL-pro-SFTPB (PS-HDL) synthesis. **B** Immunoblotting of HDL-pro-SFTPB showed that HDL successfully carried pro-SFTPB. **C** The PS-HDL treatment (100  $\mu$ g/ml, 12 h) induced M1 polarization of THP-1 derived macrophage by qPCR assay of M1/M2-associated markers. (n = 5 per group). **D** The phagocytic capability of THP-1 derived macrophages by quantifying the uptake of labeled E. coli particles after HDL and PS-HDL treatments (100  $\mu$ g/ml, 12 h), the percentage of particle-positive cells was presented as bar figure (n = 4 per group). **E** intracellular ROS release in THP-1 derived macrophages 30 min after HDL exposure was quantified via the changes in DCF fluorescence (n = 5 per group). HDL, high density lipoprotein; Pro-SFTPB, pro-pulmonary surfactant-associated protein B; C-H: control HDL; PS-HDL, Pro-SFTPB enriched HDL; TNF, tumor necrosis factor; IL-, interleukin-; MRC-1, mannose receptor C-type 1; ROS, reactive oxygen species; \*\*p < 0.01, \*\*\*p < 0.001, \*\*\*\*p < 0.0001

pathogenesis of ARDS and its clinical predictive merits for ARDS prognosis.

In this study, our results showed the correlation of HDL-pro-SFTPB with the levels of plasma cytokines and chemokines and growth factors, including IL-3/8/15/18, IP10, MCP1/3, MIG, MDC and PDGF. IP-10, also known

as C-X-C motif chemokine ligand (CXCL)10, and MIG, also known as CXCL9, are pro-inflammatory chemokines in response to interferon- $\gamma$  (IFN- $\gamma$ ) and share the same receptor: C-X-C motif receptor 3 (CXCR3) [24]. MCP-1, also known as C-C motif chemokine ligand (CCL)2, and MCP-3, also known as CCL7, are members of

CC chemokine subfamily and their receptors are C–C chemokine receptor type (CCR)2 and CCR1, respectively. The IFN- $\gamma$ -CXCL9/10-CXCR3, CCL2/CCR2, and CCL7/CCR1 signaling axis have been identified as pivotal factors in the exacerbation of sepsis-associated pathophysiological processes, facilitating the recruitment of macrophages into lung tissues and the polarization of M1 macrophage [25–30]. Our data revealed that pro-SFTPb level in HDL exhibit a significantly positive correlation with the concentrations of IP-10, MCP-1, MCP-3 and MIG, suggesting a potential role for HDL-pro-SFTPb in M1 macrophage polarization. This clinical evidence supports our *in vitro* finding that A-HDL and HDL-pro-SFTPb promoted M1 polarization of THP-1 derived macrophages. These findings suggest the monomacrophage could be the critical target of adverse HDL during the development of ARDS.

Pro-SFTPb is synthesized as a hydrophilic 42-kDa protein by type 2 alveolar pneumocytes and non-ciliated bronchiolar epithelial cells and subsequently matures into the hydrophobic form of SFTPb. Plasma fractionation analysis revealed that pro-SFTPb is almost entirely bound to HDL, as HDL acts as the primary carrier for pro-SFTPb [22, 23]. Impairment of the alveolar-capillary barrier is theorized to result in an enhanced leakage of pro-SFTPb from the lung [31]. Previous research has linked elevated plasma pro-SFTPb levels to various pulmonary disorders, suggesting its potential as a biomarker for the progression of chronic obstructive pulmonary disease, interstitial lung disease, and lung cancer [32–34]. Therefore, we hypothesize that the increase of pro-SFTPb in HDL might be due to an impaired epithelial-endothelial barrier leading to excessive pro-SFTPb binding and incorporation into HDL.

In addition, our results confirmed that free pro-SFTPb cannot promote macrophage polarization. Therefore, we hypothesize that only the incorporation of pro-SFTPb could facilitate macrophage polarization by promoting adverse HDL functional remodeling. Our *in vitro* results confirmed this hypothesis. Pro-SFTPb enriched HDL significantly promoted M1 polarization of macrophage rather than free pro-SFTPb exposure. The HDL associated with pro-SFTPb incorporation would likely account for the pro-inflammatory transition rather than the pro-SFTPb itself. Although more mechanistic studies are required to decipher the black box of the mechanisms facilitating adverse HDL remodeling, our interesting findings clearly present the importance of pro-SFTPb enriched HDL in the development of ARDS.

In the last decades, research involving studies on ARDS biomarkers and proteomics technologies has been

increasing. Proteomics has enabled the identification and quantification of numerous proteins that were difficult to detect using traditional methods and presents a novel avenue for developing diagnostic and prognostic tools, and personalized therapy in ARDS [35, 36]. Our results demonstrated that HDL-pro-SFTPb is causally involved in ARDS-related 28-day mortality by inducing M1 polarization of macrophage, and it could be a promising prognostic biomarker for septic ARDS. Furthermore, patients with sepsis are at risk of developing ARDS, and timely intervention is crucial for improving survival rates. HDL-pro-SFTPb levels could be an early predictor of disease severity, allowing clinicians to identify high-risk patients and initiate more aggressive treatment protocols early on. Since pro-SFTPb enriched HDL promotes M1 polarization of macrophages, which is linked to inflammatory lung injury in ARDS, targeting the pro-SFTPb-HDL could represent a novel therapeutic strategy. Agents, such as specific antibodies that block the interaction between HDL-pro-SFTPb and macrophages, could potentially prevent excessive inflammation and tissue damage in the lung.

## Conclusions

In conclusion, our results demonstrate that increased HDL-pro-SFTPb is clinically associated with the poor prognosis of ARDS. These findings depict the importance of HDL-pro-SFTPb in HDL pro-inflammatory transition during septic-ARDS, leading to exacerbated progression of septic-ARDS through enhancing M1 macrophage polarization.

## Abbreviations

ARDS	Acute respiratory distress syndrome
HDL	High-density lipoprotein
HDL-C	HDL-cholesterol
A-HDL	HDL from septic-ARDS patients
N-HDL	HDL from healthy controls
Apo	Apolipoprotein
PON	Paraoxonase
SAA	Serum amyloid A
IGFBP3	Insulin-like growth factor-binding protein 3
SERPINS5	Serpin family A member 5
LBP	Lipopolysaccharide-binding protein
pro-SFTPb	Pro-pulmonary surfactant-associated protein B
IMV	Invasive mechanical ventilation
RICU	Respiratory intensive care unit
BMI	Body mass index
APACHE II	Acute physiology and chronic health evaluation II
SOFA	Sequential organ failure assessment
DIA-MS	Data-independent acquisition mass spectrometry
AGC	Automatic gain control
HCD	Higher-energy collisional dissociation
PCA	Principal component analysis
DEP	Differentially expressed protein
GO	Gene Ontology Consortium
PRM	Parallel reaction monitoring
SEM	Standard error of the mean

ROC	Receiver operating characteristic
AUC	Area under the curves
HC	Healthy control
PMA	Phorbol myristate acetate
PS-HDL	Pro-SFTPB enriched HDL
MRC1	Mannose receptor C-type 1
LDH	Lactate dehydrogenase
CXCL	C-X-C motif chemokine ligand
IFN	Interferon
CXCR	C-X-C motif receptor
CCL	C-C motif chemokine ligand
CCR	C-C chemokine receptor type

## Supplementary Information

The online version contains supplementary material available at <https://doi.org/10.1186/s12967-025-06100-6>.

Supplementary materials 1.

Supplementary materials 2.

## Acknowledgements

We want to acknowledge the equipment assistance of the Institute of Genetics and Developmental Biology, Chinese Academy of Sciences.

## Author contributions

Study design and decision to submit (JJ); manuscript writing (LY and JJ); data collection and analysis (LY, ZX, FD, ZW and XS); in vitro experiments (ZX); interpretation of data: (YL and JJ); the review of this manuscript (YM and JW); All authors approved the manuscript.

## Funding

Not applicable.

## Availability of data and materials

The datasets used and/or analysed during the current study are available from the corresponding author on reasonable request.

## Declarations

### Ethics approval and consent to participate

All studies involving human samples were approved by the Ethics Committee of Beijing Chao-Yang Hospital (2021-KE-313) and Beijing Youan Hospital (approval No.: LL-2021-148-K) and informed consent for research use of samples was obtained from all subjects. All methods were carried out in accordance with relevant guidelines and regulations, including the Code of Ethics of the World Medical Association (Declaration of Helsinki).

### Consent for publication

Not applicable.

### Competing interests

The authors declare that they are no conflicts of interest.

### Author details

<sup>1</sup>Department of Respiratory and Critical Care Medicine, Beijing Institute of Hepatology, Beijing Youan Hospital, Capital Medical University, No.8 Xi Tou Tiao, Youanmen Wai, Beijing, China. <sup>2</sup>Department of Respiratory and Critical Care Medicine, Beijing Institute of Respiratory Medicine, Beijing Chaoyang Hospital, Capital Medical University, NO.5 Jingyuan Road, Beijing, China. <sup>3</sup>Medical Research Center, Beijing Institute of Respiratory Medicine, Beijing Chaoyang Hospital, Capital Medical University, NO.5 Jingyuan Road, Beijing, China.

Received: 19 October 2024 Accepted: 8 January 2025

Published online: 16 January 2025

## References

- Bos LDJ, Ware LB. Acute respiratory distress syndrome: causes, pathophysiology, and phenotypes. *Lancet*. 2022;400(10358):1145–56.
- Rigamonti A, Villar J, Segura E. Monocyte differentiation within tissues: a renewed outlook. *Trends Immunol*. 2023;44(12):999–1013.
- Chen X, Tang J, Shuai W, Meng J, Feng J, Han Z. Macrophage polarization and its role in the pathogenesis of acute lung injury/acute respiratory distress syndrome. *Inflamm Res*. 2020;69(9):883–95.
- Wang A, Kang X, Wang J, Zhang S. IFIH1/IRF1/STAT1 promotes sepsis associated inflammatory lung injury via activating macrophage M1 polarization. *Int Immunopharmacol*. 2023;114: 109478.
- Wang Z, Wang Z. The role of macrophages polarization in sepsis-induced acute lung injury. *Front Immunol*. 2023;14:1209438.
- Morrell ED, Bhatraju PK, Mikacenic CR, Radella F 2nd, Manicone AM, Stapleton RD, Wurfel MM, Gharib SA. Alveolar macrophage transcriptional programs are associated with outcomes in acute respiratory distress syndrome. *Am J Respir Crit Care Med*. 2019;200(6):732–41.
- Eckardstein AV, Nordestgaard BG, Remaley AT, Catapano AL. High-density lipoprotein revisited: biological functions and clinical relevance. *Eur Heart J*. 2023;44(16):1394–407.
- De Nardo D, Labzin LI, Kono H, Seki R, Schmidt SV, Beyer M, Xu D, Zimmer S, Lahrmann C, Schildberg FA, Vogelhuber J, Kraut M, Ulas T, Kerksiek A, Krebs W, Bode N, Grebe A, Fitzgerald ML, Hernandez NJ, Williams BRG, Knolle P, Kneilling M, Röcken M, Lütjohann D, Wright SD, Schultze JL, Latz E. High-density lipoprotein mediates anti-inflammatory reprogramming of macrophages via the transcriptional regulator ATF3. *Nat Immunol*. 2014;15(2):152–60.
- Lee MKS, Moore X-L, Fu Y, Al-Sharea A, Dragoljevic D, Fernandez-Rojo MA, Parton R, Sviridov D, Murphy AJ, Chin-Dusting JPF. High-density lipoprotein inhibits human M1 macrophage polarization through redistribution of caveolin-1. *Br J Pharmacol*. 2016;173(4):741–51.
- Chien JY, Jerng JS, Yu CJ, Yang PC. Low serum level of high-density lipoprotein cholesterol is a poor prognostic factor for severe sepsis. *Crit Care Med*. 2005;33(8):1688–93.
- Yang L, Luo Z, Shi X, Pang B, Ma Y, Jin J. Different value of HDL-C in predicting outcome of ARDS secondary to bacterial and viral pneumonia: a retrospective observational study. *Heart Lung*. 2021;50(1):206–13.
- Tanaka S, Couret D, Tran-Dinh A, Duranteau J, Montravers P, Schwendeman A, Meilhac O. High-density lipoproteins during sepsis: from bench to bedside. *Crit Care*. 2020;24(1):134.
- Guirgis FW, Dodani S, Moldawer L, Leeuwenburgh C, Bowman J, Kalynych C, Jones AE, Reddy ST, Moore FA. Exploring the predictive ability of dysfunctional high-density lipoprotein for adverse outcomes in emergency department patients with sepsis: a preliminary investigation. *Shock*. 2017;48(5):539–44.
- Tanaka S, Diallo D, Delbosq S, Geneve C, Zappella N, Yong-Sang J, Patche J, Harrois A, Hamada S, Denamur E, Montravers P, Duranteau J, Meilhac O. High-density lipoprotein (HDL) particle size and concentration changes in septic shock patients. *Ann Intens Care*. 2019;9(1):68.
- Yang L, Liu S, Han S, Hu Y, Wu Z, Shi X, Pang B, Ma Y, Jin J. The HDL from septic-ARDS patients with composition changes exacerbates pulmonary endothelial dysfunction and acute lung injury induced by cecal ligation and puncture (CLP) in mice. *Respir Res*. 2020;21(1):293.
- Vaisar T, Pennathur S, Green PS, Gharib SA, Hoofnagle AN, Cheung MC, Byun J, Vuletic S, Kassim S, Singh P, Chea H, Knopp RH, Brunzell J, Geary R, Chait A, Zhao X-Q, Elkon K, Marcovina S, Ridker P, Oram JF, Heinecke JW. Shotgun proteomics implicates protease inhibition and complement activation in the antiinflammatory properties of HDL. *J Clin Investig*. 2007;117(3):746–56.
- Davidson WS, Shah AS, Sexmith H, Gordon SM. The HDL proteome watch: compilation of studies leads to new insights on HDL function. *Biochim Biophys Acta Mol Cell Biol Lipids*. 2022;1867(2): 159072.
- Chiesa ST, Charakida M. High-density lipoprotein function and dysfunction in health and disease. *Cardiovasc Drugs Ther*. 2019;33(2):207–19.
- Souza Junior DR, Silva ARM, Rosa-Fernandes L, Reis LR, Alexandria G, Bhosale SD, Ghilardi FR, Dalcoquio TF, Bertolin AJ, Nicolau JC, Marinho CRF, Wrenger C, Larsen MR, Siciliano RF, Di Mascio P, Palmisano G, Ronsein GE. HDL proteome remodeling associates with COVID-19 severity. *J Clin Lipidol*. 2021;15(6):796–804.
- Cardner M, Yalcinkaya M, Goetze S, Luca E, Balaz M, Hunjadi M, Hartung J, Shemet A, Kränkel N, Radosavljevic S, Keel M, Othman A, Karsai G,

- Hornemann T, Claassen M, Liebisch G, Carreira E, Ritsch A, Landmesser U, Krützfeldt J, Wolfrum C, Wollscheid B, Beerwinkel N, Rohrer L, von Eckardstein A. Structure-function relationships of HDL in diabetes and coronary heart disease. *JCI Insight*. 2020;5(1):e131491.
21. Chung BH, Wilkinson T, Geer JC, Segrest JP. Preparative and quantitative isolation of plasma lipoproteins: rapid, single discontinuous density gradient ultracentrifugation in a vertical rotor. *J Lipid Res*. 1980;21(3):284–91.
  22. Shao B, Snell-Bergeon JK, Pyle LL, Thomas KE, de Boer IH, Kothari V, Segrest J, Davidson WS, Bornfeldt KE, Heinecke JW. Pulmonary surfactant protein B carried by HDL predicts incident CVD in patients with type 1 diabetes. *J Lipid Res*. 2022;63(4): 100196.
  23. Banfi C, Brioschi M, Karjalainen MK, Huusko JM, Gianazza E, Agostoni P. Immature surfactant protein-B impairs the antioxidant capacity of HDL. *Int J Cardiol*. 2019;285:53–8.
  24. Álvarez H, Gutiérrez-Valencia A, Mariño A, Saborido-Alconchel A, Calderón-Cruz B, Pérez-González A, Alonso-Domínguez J, Martínez-Barros I, Gallego-Rodríguez M, Moreno S, Aldamiz T, Montero-Alonso M, Bernal E, Galera C, Llibre JM, Poveda E. IP-10 and MIG are sensitive markers of early virological response to HIV-1 integrase inhibitors. *Front Immunol*. 2023;14:1257725.
  25. Herzig DS, Luan L, Bohannon JK, Toliver-Kinsky TE, Guo Y, Sherwood ER. The role of CXCL10 in the pathogenesis of experimental septic shock. *Crit Care*. 2014;18(3):R113.
  26. Wang J, Chen G, Li L, Luo S, Hu B, Xu J, Luo H, Li S, Jiang Y. Sustained induction of IP-10 by MRP8/14 via the IFN $\beta$ -IRF7 axis in macrophages exaggerates lung injury in endotoxemic mice. *Burns Trauma*. 2023;11:tkad006.
  27. Zhou C, Shen Z, Shen B, Dai W, Sun Z, Guo Y, Xu X, Wang J, Lu J, Zhang Q, Luo X, Qu Y, Dong H, Lu L. FABP4 in LSECs promotes CXCL10-mediated macrophage recruitment and M1 polarization during NAFLD progression. *Biochim Biophys Acta Mol Basis Dis*. 2023;1869(7): 166810.
  28. Ma P, Liu J, Qin J, Lai L, Heo GS, Luehmann H, Sultan D, Bredemeyer A, Bajapa G, Feng G, Jimenez J, He R, Parks A, Amrute J, Villanueva A, Liu Y, Lin C-Y, Mack M, Amancherla K, Moslehi J, Lavine KJ. Expansion of pathogenic cardiac macrophages in immune checkpoint inhibitor myocarditis. *Circulation*. 2024;149(1):48–66.
  29. Ni J, Guo T, Zhou Y, Jiang S, Zhang L, Zhu Z. STING signaling activation modulates macrophage polarization via CCL2 in radiation-induced lung injury. *J Transl Med*. 2023;21(1):590.
  30. Xie C, Ye F, Zhang N, Huang Y, Pan Y, Xie X. CCL7 contributes to angiotensin II-induced abdominal aortic aneurysm by promoting macrophage infiltration and pro-inflammatory phenotype. *J Cell Mol Med*. 2021;25(15):7280–93.
  31. Palaniyar N, Gargiulo P, Banfi C, Ghilardi S, Magri D, Giovannardi M, Bonomi A, Salvioni E, Battaia E, Filardi PP, Tremoli E, Agostoni P. Surfactant-derived proteins as markers of alveolar membrane damage in heart failure. *PLoS ONE*. 2014;9(12): e115030.
  32. Enomoto T, Shirai Y, Takeda Y, Edahiro R, Shichino S, Nakayama M, Takahashi-Itoh M, Noda Y, Adachi Y, Kawasaki T, Koba T, Futami Y, Yaga M, Hosono Y, Yoshimura H, Amiya S, Hara R, Yamamoto M, Nakatsubo D, Suga Y, Naito M, Masuhiro K, Hirata H, Iwahori K, Nagatomo I, Miyake K, Koyama S, Fukushima K, Shiroyama T, Naito Y, Futami S, Natsume-Kitatani Y, Nojima S, Yanagawa M, Shintani Y, Nogami-Itoh M, Mizuguchi K, Adachi J, Tomonaga T, Inoue Y, Kumanogoh A. SFTPB in serum extracellular vesicles as a biomarker of progressive pulmonary fibrosis. *JCI Insight*. 2024;9(11): e177937.
  33. Leung JM, Mayo J, Tan W, Tammemagi CM, Liu G, Peacock S, Shepherd FA, Goffin J, Goss G, Nicholas G, Tremblay A, Johnston M, Martel S, Laberge F, Bhatia R, Roberts H, Burrowes P, Manos D, Stewart L, Seely JM, Gingras M, Pasion S, Tsao MS, Lam S, Sin DD. Pan-canadian early lung cancer study G Plasma pro-surfactant protein B and lung function decline in smokers. *Eur Respir J*. 2015;45(4):1037–45.
  34. Sin DD, Tammemagi CM, Lam S, Barnett MJ, Duan X, Tam A, Auman H, Feng Z, Goodman GE, Hanash S, Taguchi A. Pro-surfactant protein B as a biomarker for lung cancer prediction. *J Clin Oncol*. 2013;31(36):4536–43.
  35. Battaglini D, Al-Husinat LI, Normando AG, Leme AP, Franchini K, Morales M, Pelosi P, Rocco PRM. Personalized medicine using omics approaches in acute respiratory distress syndrome to identify biological phenotypes. *Respirat Res*. 2022;23(1):318.
  36. Nie X, Qian L, Sun R, Huang B, Dong X, Xiao Q, Zhang Q, Lu T, Yue L, Chen S, Li X, Sun Y, Li L, Xu L, Li Y, Yang M, Xue Z, Liang S, Ding X, Yuan C, Peng L, Liu W, Yi X, Lyu M, Xiao G, Xu X, Ge W, He J, Fan J, Wu J, Luo M, Chang X, Pan H, Cai X, Zhou J, Yu J, Gao H, Xie M, Wang S, Ruan G, Chen H, Su H, Mei H, Luo D, Zhao D, Xu F, Li Y, Zhu Y, Xia J, Hu Y, Guo T. Multi-organ proteomic landscape of COVID-19 autopsies. *Cell*. 2021;184(3):775–791. e714.

## Publisher's Note

Springer Nature remains neutral with regard to jurisdictional claims in published maps and institutional affiliations.